OLD MAIN-SEQUENCE TURNOFF PHOTOMETRY IN THE SMALL MAGELLANIC CLOUD. II. STAR FORMATION HISTORY AND ITS SPATIAL GRADIENTS

Noelia E. D. Noël

Instituto de Astrofísica de Canarias. 38200 La Laguna. Tenerife, Canary Islands, Spain.

noelia@roe.ac.uk

Antonio Aparicio

Instituto de Astrofísica de Canarias. 38200 La Laguna. Tenerife, Canary Islands, Spain.

Carme Gallart

Instituto de Astrofísica de Canarias. 38200 La Laguna. Tenerife, Canary Islands, Spain.

Sebastián L. Hidalgo

Instituto de Astrofísica de Canarias. 38200 La Laguna. Tenerife, Canary Islands, Spain.

Edgardo Costa

Universidad de Chile, Departamento de Astronomía, Casilla 36-D, Santiago, Chile.

and

René A. Méndez

Universidad de Chile, Departamento de Astronomía, Casilla 36-D, Santiago, Chile.

ABSTRACT

We present a quantitative analysis of the star formation history (SFH) of 12 fields in the Small Magellanic Cloud (SMC) based on unprecedented deep [(B-R),R] color-magnitude diagrams (CMDs). Our fields reach down to the oldest main sequence (MS) turnoff with high photometric accuracy, which is vital for obtaining accurate SFHs, particularly at intermediate and old ages. We use the IAC-pop code to obtain the SFH, using a single CMD generated using IAC-star. We obtain the SFH as a function $\psi(t, z)$ of age and metallicity. We also consider several auxiliary functions: The Initial Mass Function (IMF), $\phi(m)$, and

a function accounting for the frequency and relative mass distribution of binary stars, $\beta(f, q)$. We find that there are four main periods of enhancement of star formation: a young one peaked at ∼0.2-0.5 Gyr old, only present in the eastern and in the central-most fields; two at intermediate ages present in all fields (a conspicuous one peaked at ∼4-5 Gyr old, and a less significant one peaked at ∼1.5-2.5); and an old one, peaked at ∼10 Gyr in all fields but the western ones. In the western fields, this old enhancement splits into two, one peaked at ∼8 Gyr old and another at ∼12 Gyr old. This "two-enhancement" zone seems to be a robust feature since it is unaffected by our choice of stellar evolutionary library but more data covering other fields of the SMC are necessary in order to ascertain its significancy.

Correlation between the star formation rate enhancements and SMC-Milky Way encounters is not clear. Some correlation could exist with encounters taken from the orbit determination of Kallivayalil, van der Marel, & Alcock (2006). But our results would be also fit in a first pericenter passage scenario like the one claimed by Besla et al. (2007). For SMC-Large Magellanic Cloud (LMC) encounters, we find a correlation only for the most recent encounter ∼0.2 Gyr ago. This coincides with the youngest $\psi(t)$ enhancement peaked at these ages in our eastern fields.

The population younger than 1 Gyr old in the wing area represents ∼7-12% of the total $\psi(t)$. This does not reflect an exceptional increment in the present star formation as compared with the average $\psi(t)$ but it is very significant in the sense that these eastern fields are the only ones of this study in which star formation is currently going on. There is a strong dichotomy between East/Southeast and West in the current irregular shape of the SMC. We find that this dichotomy is produced by the youngest population and began ∼1.0 Gyr ago or later.

The age of the old population is similar at all radii and at all azimuth and we constrain the age of this oldest population to be older than ∼12 Gyr old. We do not find yet a region dominated by an old, Milky Way-like, halo at 4.5 kpc from the SMC center, indicating either that this old stellar halo does not exist in the SMC or that its contribution to the stellar populations, at the galactocentric distances of our outermost field, is negligible. Finally, we derive the age-metallicity relation and find that, in all fields, the metallicity increased continuously from early epochs until the present. This is in good agreement with the results from the CaII triplet, a completely independent method, constituting external consistency proof of IAC-pop in determining the chemical enrichment law.

Subject headings: local group galaxies: evolution — galaxies: individual (SMC) — galaxies: photometry — galaxies: stellar content

1. INTRODUCTION

The Local Group dwarf galaxies provide a unique laboratory for studying and testing galaxy formation theories and cosmology. Their close proximity allows individual stars to be resolved, giving accurate kinematics (see e.g. Walker et al. 2006), photometry (see e.g. Noël et al. 2007, hereafter Paper I) and spectroscopy (e.g. Carrera et al. 2008a). Their stellar populations can be characterized in detail and their star formation histories (SFHs) derived (e.g. Gallart et al. 1999). Their extended edges can be compared with cosmological predictions to give useful constraints (e.g. Noël & Gallart 2007); and their large mass-to-light ratios can be used, through dynamical modelling, to place constraints on the nature of dark matter (e.g. Kleyna et al. 2001).

Containing stars born over the whole lifetime of a galaxy, the color magnitude diagram (CMD) is a fossil record of the SFH. For the Milky Way satellites, it is possible to obtain accurate SFHs, from CMDs reaching the oldest main-sequence (MS) turnoffs, using ground-based telescopes. Reaching the oldest MS turnoffs is vital for breaking the age-metallicity degeneracy and properly characterising the intermediate-age and old population (see Gallart, Zoccali, & Aparicio 2005). The Magellanic Clouds (MCs), our nearest irregular satellites, provide an ideal environment for this work. In this paper, we focus on the Small Magellanic Cloud (SMC). The SMC has been historically neglected in favor of its larger neighbor, the Large Magellanic Cloud (LMC). However, recently there has been growing interest in the SMC as a result of new proper motion measurements –which constrain the past orbital motions of the MCs (Kallivayalil et al. 2006; Piatek et al. 2008; Costa et al. 2009). These indicate that it may have a different origin to the LMC (see e.g. Bekki et al. 2004). If true, this would imply that its SFH, evolution and structure could differ significantly from that of the LMC.

The SMC lies at a distance of 61.1 kpc from the sun (Westerlund 1997; Storm et al. 2004; Hilditch, Howarth, & Harries 2005; Keller & Wood 2006), has a mass interior to 3 kpc of $M_{SMC}\sim3\times10^9 M_\odot$ (Harris & Zaritsky 2006), a high fraction of HI ($M_{HI}\sim4\times10^8 M_\odot$, Stanimirovič et al. 1999), a luminosity of 6×10^8 $L_\odot$ in the *V*-band (de Vaucouleurs et al. 1991), and a current metallicity of ∼1/5 solar (Dufour 1975; Peimbert & Torres-Peimbert 1976; Dufour & Harlow 1977; Peimbert, Peimbert, & Ruiz 2000). The SMC is actively forming stars at a global rate of $0.05 M_\odot$/yr (Wilke et al. 2004), and is populated by well-studied HII regions and star clusters of all ages (e.g. Massey 2002; Rafelski & Zaritsky 2005;

Chiosi et al. 2006; Bica et al. 2008; Piatti et al. 2008; Glatt et al. 2008b).

1.1. The SMC stellar content from field stars

The most comprehensive study of the SFH of the SMC to date was presented by Harris & Zaritsky (2004; hereafter HZ04)[1]. They derived the global SFH of the SMC, based on the Magellanic Clouds Photometric Survey (MCPS; Zaritsky et al. 1997) *UBVI* catalog that includes over 6 million SMC stars. They used the StarFISH package (Harris & Zaritsky 2001) to determine the global SFH of the SMC, derived by summing the star formation rate (SFR) over all 351 subregions and using three different metallicities. They found that there was a significant epoch of star formation up to 8.4 Gyr ago when ∼50% of the stars were formed, followed by a long quiescent period in the range 3 Gyr≤age≤8.4 Gyr, and a more or less continuous period of star formation starting 3 Gyr ago and extending to the present. They also found three peaks in the SFR, at 2-3 Gyr, at 400 Myr, and 60 Myr ago.

While global studies of the SMC like HZ04 are invaluable in aiding our understanding of the evolution of the SMC, their CMDs do not go deep enough to derive the full SFH from the information on the MS (B∼22, corresponding to stars younger than ∼3 Gyr old on the main sequence). Obtaining CMDs reaching the oldest MS turnoff is essential in order to properly constrain the intermediate-age and old population (e.g. see Paper I; Gallart, Zoccali, & Aparicio 2005, for a review). Going deep usually means sacrificing the available field of view so such studies are very complementary to galaxy-wide surveys like HZ04. To our knowledge, the papers which have presented CMDs reaching the oldest MS turnoffs so far, studying a small field of view are: Dolphin et al. (2001), McCumber et al. (2005), and Chiosi & Vallenari (2007). Dolphin et al. (2001) presented a combination of HST and ground-based V and I images of a SMC field situated 2° northeast of NGC 121. Using the ground-based CMD (for statistical reasons), with the Girardi et al. (2000) models, they quantitatively determined the SFH for that field and found a broadly peaked SFH, with the largest star formation rate occuring between 5 and 8 Gyr ago, and some small amount of star formation going on since a very early epoch and down to $\simeq$ 2 Gyr ago. McCumber et al. (2005) analyzed the stellar populations of a SMC field located in the wing area with observations from the HST WFPC2. They compared the luminosity function from their observed CMD with those obtained from two different model CMDs, one with constant $\psi(t)$

[1]Many other recent studies have also made valuable contributions. For example, Cioni et al. (2006) compared the k magnitude distribution of the SMC asymptotic giant branch stars obtained from DENIS and 2MASS data with theoretical distributions. They found that the SMC is on average 7-8 Gyr old, but that there are older stars present at its periphery while younger stars are located towards the LMC.

and another with bursts of star formation at ∼2 and at ∼8 Gyr. They found that the population appears to have formed largely in a quasi-continuous mode, with a main period of star formation between 4 and 12 Gyr ago and a very prominent recent star formation event producing bright stars as young as 100±10 Myr. Using deep CMDs obtained with the ACS, Chiosi & Vallenari (2007) retrieved the SFH of three fields around SMC clusters. The fields are located at galactocentric distances of ∼0.22 kpc and ∼0.45 kpc toward the East, and at ∼0.9 kpc in the southern direction. Chiosi & Vallenari found two main episodes in the SFR, at 300-400 Myr and between 3 Gyr and 6 Gyr. They also found that the SFR was low until ∼6 Gyr ago, when few stars were formed.

1.2. The Stellar Populations of the outer reaches of the SMC

Photometric studies of the outer SMC began with the pioneering work of Gardiner & Hatzidimitriou (1992). With a rather shallow photometry (reaching the horizontal branch (HB) level at R∼20 mag), they mainly gave information about the young populations (age ≤2 Gyr). From their CMDs and contour plots of the surface distribution of MS stars with B-R<0.1 and R<20, they noticed the almost complete absence of bright MS stars in the northwestern part, while a considerable bright MS population was present in the eastern and southern area. With the aid of luminosity functions they found that young populations (<0.6 Gyr in age) are concentrated towards the center of the SMC and in the "wing"[2] region. Using an index defined as the difference between the median color [in (B-R)] of the red clump (RC) and the color of the red giant branch (RGB) at the level of the HB, the authors inferred that the bulk of the field population has a median age around 10-12 Gyr.

More recently, Harris (2007) presented the SFH of the young inter-Cloud population along the ridgeline of the HI gas that forms the Magellanic Bridge and found an intermediate-age and old population at 4.4° and 4.9° from the SMC center in that direction, but only a young population belonging to the SMC at 6.4° (∼7.2 kpc). At the same time, Noël & Gallart (2007), presented the analysis of three SMC fields, located in the southern outskirts of the SMC. They found the first evidence of intermediate-age and old stars belonging to the SMC at 5.8° (6.5 Kpc) from the SMC center. These studies together suggest that the SMC is more extended than previously thought.

[2]The wing is located in the eastern side of the SMC, facing the LMC.

1.3. Context of the present work

In Paper I, we presented the isochrones and color functions analysis of twelve unprecedented deep *BR*-based SMC CMDs corresponding to fields ranging from ∼1° (∼1.1 kpc) to ∼4° (∼4.5 kpc) from the SMC center. The fields are distributed in different parts of the SMC, avoiding the central area (see figure 1). Each field reaches down to the old MS turnoffs, allowing for a good characterisation of the intermediate-age and old population in these areas. The western fields contain very few stars younger than ∼3 Gyr, while the fields located towards the east –the wing region– show very active current star formation. The presence of considerable amounts of young population in the eastern fields and lack thereof in the western ones is in good correspondence with the existence or absence of large amounts of HI at the corresponding locations (Stanimirovič et al. 1999). A significant intermediate-age population is present in all of our fields.

In this paper, we extend the analysis presented in Paper I and obtain quantitative SFHs of all the analyzed fields using the IAC-pop code (Aparicio & Hidalgo 2009). IAC-pop allows us to compare the observed CMD with synthetic CMDs generated using IAC-star (Aparicio & Gallart 2004). To compute the synthetic CMDs, suitable stellar evolution libraries and ingredientes were adopted.

The SFH of the SMC as derived from CMDs that reach the oldest MS turnoffs allows us to address several important questions, also posed in paper I: (i) What is the age distribution of the old and intermediate-age population?; (ii) Are there gradients in the composition of this underlying population?; and (iii) Shallower studies inform us about the young population, but does this young population reflect an exceptional increase of the star formation at the present time with respect to the average SFR?

This paper is organized as follows. In § 2, we briefly summarize the characteristics of the SMC data. In § 3, we explain the procedure we followed to quantitatively retrieve the SFH. In § 4, we discuss the ingredients of our models, such as the input stellar evolution models, the IMF, the characteristics of the binary star population, and the parameterization of the SFH, among others. In § 5, we present the detailed SFH of our SMC fields. Finally, in § 6 we discuss our results and present our conclusions.

2. The SMC data

B and *R* band images of twelve 8.85′×8.85′ SMC fields were obtained throughout a four year campaign (2001-2004) using the 100-inch telescope at Las Campanas Observatory (see figure 1). Photometry of the stars in all the SMC fields was obtained using the set of

DAOPHOT, ALLSTAR, and ALLFRAME programs (Stetson 1994) and the final photometry was calibrated to the Johnson-Cousins system. A total of 215,121 stars down to $R{\sim}24$ were kept, with small photometric errors ($\sigma{\leq}0.15$, $CHI{\leq}2.5$, and $-0.6{\leq}SHARP{\leq}0.6$). See Paper I for a complete description of the data reduction and photometry.

3. Deriving the SFH of a system

The first step in accurately determining the SFH of a system is a deep CMD reaching the oldest MS turnoffs. The advantage of reaching the oldest MS turnoffs is twofold: (i) stellar evolution models are more accurate along the MS than for for more advanced stellar evolutionary phases such as the RGB or the HB where the corresponding physics is more complicated or uncertain; and (ii) stars are less densely packed on the MS than in the RGB or HB where stars of very different ages are packed together in the CMD in a small interval of color and/or magnitude, and suffer from important age-metallicity degeneracies. The SFH is composed of several pieces of information. We adopt here the approach of Aparicio & Hidalgo (2009), which can be sketched as follows: since time and metallicity are the most important variables in the problem, we define the SFH as a function $\psi(t, z)$ such that $\psi(t, z)\mathrm{d}t\mathrm{d}z$ is the number of stars formed at time t' in the interval $t < t' \leq t + \mathrm{d}t$ and with metallicity z' in the interval $z < z' \leq z + \mathrm{d}z$. Where necessary, the function $\psi(t)$ –defined as an integral over metallicity of $\psi(t, z)$– and the function $\psi(z)$ –defined as an integral over time of $\psi(t, z)$– will be used to represent the time-dependent SFH and metallicity-dependent SFH, respectively. There are also several other functions and parameters related to the SFH, that we will consider here as auxiliary: the Initial Mass Function (IMF), $\phi(m)$; and a function accounting for the frequency, f, and relative mass distribution, q, of binary stars, $\beta(f, q)$, are the main ones. Our results are not sensitive to our assumptions for $\phi(m)$ and $\beta(f, q)$. Other parameters affecting the solution of $\psi(t, z)$ are the distance and reddening (including differential reddening) adopted. For a detailed discussion, see Aparicio & Hidalgo (2009) and Hidalgo et al. (2009).

An important limitation on the information that can be retrieved from the empirical data, is produced by observational effects. These include all the factors affecting and distorting the CMD, namely the signal-to-noise limitations, the defects of the detector and the crowding and blending between stars. The consequences are a loss of stars, changes in measured stellar colors and magnitudes, and external errors, which are usually larger and more difficult to control than internal ones (Aparicio & Gallart 1995). A realistic simulation of observational effects is necesary in order to obtain an accurate solution for $\psi(t, z)$. In our case, the simulation of the observational effects in the synthetic CMDs was performed

on a star-by-star basis, using an empirical approach that makes no assumption about the nature of the errors or about their propagation (Aparicio & Gallart 1995). Once the errors in the synthetic CMD are simulated, we call it *model* CMD. The process is fully described in Gallart et al. (1999, and references therein) and in Paper I.

The procedure followed to find the SFH is similar to that described in Hidalgo et al. (2009). The SFH is derived through a comparison of the distribution of stars in the observed CMD with that of a model CMD, using the IAC-pop code (Aparicio & Hidalgo 2009). A single *global* synthetic CMD was generated using the IAC-star code for each set of input parameters. This global synthetic CMD comprises 10^6 stars with ages and metallicities uniformly distributed over the full interval of variation of $\psi(t, z)$ in time and metallicity. This represents a constant SFR as a function of time with equally probable metallicity, within a given range, for each age (see § 4). Observational effects were simulated in the global synthetic CMD as mentioned above. The synthetic stars were distributed in an array of *partial models*, ψ_i , each containing stars within small intervals of age and metallicity. Then, a set of boxes was defined in the CMDs. In practice, two approaches may be used: an uniform grid and an "*à la carte*" grid (see § 4). An array, M_i^j, containing the number of stars from partial model i populating box j is computed. The same operation is made in the observed CMD, producing a vector, O^j, containing the number of observed stars in box j. This step defines the parameterization of the CMD.

Any SFH (with the restriction in time and metallicity resolution imposed by the partial models) can be written as:

$$\psi(t, z) = A \sum_i \alpha_i \psi_i \tag{1}$$

where $\alpha_i \geqslant 0$ and A is a scaling constant. The asociated distribution of stars in the defined boxes is

$$M^j = A \sum_i \alpha_i M_i^j \tag{2}$$

M_i can now be compared with O^j using a merit function. A reduced Mighell χ^2 (Mighell 1999), $\chi^2_\nu = \chi^2/\nu$ is used, where $\nu = k - 1$ is the number of degrees of freedom, and k is the number of boxes used to parameterize the CMD. Minimization of χ^2_ν with respect to the α_i coeficients provides the best solution as well as a test on whether it is acceptable, and a way to estimate errors for the solution. IAC-pop makes use of a genetic algorithm for the minimization of χ^2_ν. Considering the large number of dimensions of the problem ($n \times m$, n

age intervals and m metallicity intervals), such an efficient solving procedure is required.

4. Retrieving the SFHs for the SMC fields

We used IAC-pop (Aparicio & Hidalgo 2009) to obtain the SFH, $\psi(t, z)$, in our SMC fields. For the stellar evolution libraries, we used the overshooting BaSTI[3] (Pietrinferni et al. 2004; 2006; see also Cordier et al. 2007) and Padua (summarized in Bertelli et al. 1994). Bolometric corrections from Castelli & Kurucz (2003) were adopted. The input SFR, $\psi(t)$, was chosen to be constant between 13 Gyr ago[4] and now. Kroupa's revised IMF[5], $\phi(m)$, was used (Kroupa et al. 2003). We assumed a low metallicity bound $z_i = 0.0001$, since it is compatible with the CMD and is the lowest metallicity allowed by the models. The high metallicity bound was taken from the HII region observations (Dufour 1984) (see below and table 3). It is not possible to uniquely determine the binary fraction, but we explored the consequences of the presence of binaries with properties similar to those observed locally on the CMDs of the SMC. Only in binaries with mass ratios q close to unity would the secondary have a substantial effect on the combined luminosity of the binary. For this reason, in our final models we have considered mass ratios in the interval $0.7 \lesssim q \lesssim 1.0$ (see Gallart et al. 1999 for details). After testing different binary fractions, we found that, in general, the $\psi(t, z)$ is not significantly affected by changes in $\beta(f, q)$. In our final models we considered a 30% of binary fraction. Finally, in order to obtain the global model CMD, we simulated the observational errors as mentioned in § 3. We used a distance modulus of $(m - M)_0 = 18.9$ and the reddening values given in table 1 (see Paper I for details on the reddening determinations).

Each model CMD was divided into partial models, using the age-metallicity pairs defined in tables 2, 3, and 4. In table 2, the name of each set of age intervals is shown in the first column and the sampling of such intervals is presented in the second column. Three different

[3]While finishing the present paper, the BaSTI group found that the stellar models for masses between $1.1 M_\odot$ and $2.5 M_\odot$ (i.e. age range $\simeq$ 1.0-4.0 Gyr) were calculated using an outdated version of the code. The SFHs presented here (as well as the calculations based on them) were obtained using the new version of BaSTI (see Appendix **??**).

[4]The results from the WMAP (Spergel et al. 2003) imply that the age of the universe is 13.7±0.2 Gyr. The first stars started forming ∼0.4 Gyr after the beginning of the Universe. With the current most commonly accepted distance scale for globular clusters (Carretta et al. 2000), the age of the oldest globular cluster in the Milky Way, derived using up to date stellar evolution models, is in good agreement with the age of the Universe.

[5]$m^{-1.3}$ for $0.1 \leqslant m/M_\odot < 0.5$ and $m^{-2.3}$ for $0.5 \leqslant m/M_\odot < 100$.

set of age intervals were used in order to address how the SFH is affected by changes in such age intervals. In table 3, the name of each set of metallicity intervals is shown in the first column and the sampling of such intervals is presented in the second column. The two different sets of metallicity intervals were chosen according to the stellar population present in each field. In those fields in which there is a considerable amount of young stars (eastern fields and the two closest southern ones), the metal-1 set of intervals from table 3 was used (which reaches higher metallicities), while in those in which the recent star formation is negligible, metal-2 from table 3 was used. Table 4 defines the combination of intervals of age and metallicity used for each field. The first column gives the number of simple populations; the second and third columns denote the number of age and metallicity intervals, respectively; and in the fourth column, the corresponding fields are shown. The age intervals are defined such that they are larger towards older ages. This is because older stars are more densely packed in the CMD and the isochrones become closer together as they get older, while stars have higher photometric errors at fainter magnitudes. By choosing these intervals of age for the partial models, we are introducing an upper limit to the resolution in age of $\psi(t)$.

The next step was the parameterization of the data. Instead of using an uniform grid, it is better to use one in which the box is different across the CMD. We call this "*à la carte*" parameterization (see Hidalgo et al. 2009). In this way, regions for which stellar positions as function of mass, age and metallicity, as provided by the stellar evolution theory, are better known, are sampled with smaller boxes, so receiving a larger weight in the solution searching. We performed several tests using different "*à la carte*" parameterizations. Figure 2 shows some examples of the parameterizations we performed and their corresponding solutions for $\psi(t, z)$ for field smc0057. As seen from the figures, the different SFHs are very similar and the resulting $\chi^2_{\nu,min}$ are very good in all cases, implying that the parameterization is not significatively affecting the solution. We kept the "*à la carte*" parameterization shown in figure 3(a), which has small boxes in the regions in which the stellar evolutionary phases are well known (MS), and larger boxes in the regions of the CMD in which stars in more advanced phases are located. The solution for the $\psi(t, z)$ in field smc0057 is shown in figure 3(b).

For all fields, we retrieved the SFH using both stellar evolution libraries as inputs of IAC-star: BaSTI and Padua. The results are presented in section 5.

4.1. Testing the pipeline: recovering the SFH of "mock" galaxies

Several tests of IAC-pop are discussed by Aparicio & Hidalgo (2009) and by Hidalgo et al. (2009). We have performed some more tests for our particular case, setting out to recover the SFH of two "mock" galaxies, generated using the IAC-star code. One mock

galaxy assumed a constant $\psi(t)$=1 and a metallicity law $\psi(z)$ suitable for our SMC fields (the "SMC-mock"; see below and Carrera et al. 2008b). The other assumed the same $\psi(t)$ but a different $\psi(z)$, in order to investigate if the assumption of a given metallicity law affects the results (the "metal-mock"). In both cases, 500,000 stars were considered. We simulated observational errors for each synthetic population as described in § 3. Errors from the observed field qj0116 were simulated since it is a typical "wing" field, with a fairly large amount of stars. The same test was performed simulating observational errors from other fields, obtaining similar results.

Different subsamples were extracted randomly from SMC-mock. In each case, $\psi(t)$ was recovered using a global synthetic CMD with 10^6 stars computed assuming exactly the same inputs of binariety, IMF, stellar evolution library, and bolometric corrections as the SMC-mock. The metallicity distribution was assumed equally probable between $z = 0.0001$ and $z = 0.02$, for the whole age interval. The resultant $\psi(t)$ are displayed in figure 4. Note that they deviate from the input $\psi(t)$=1 by up to 25%, showing "wiggles" with similar patterns in the different subsamples. This shows that the effect is a *systematic* error, rather than a random one. It is worth noting that this effect is not caused by the crowding present in the different fields, as shown in figure 5. This figure shows the SFH derived for SMC-mock (for the age interval age-1 from table 2) obtained after simulating the observational effects from three fields located at different galactocentric distances: the central-most field, smc0057 (located at ∼1.1 kpc), the outer-most one (at ∼4.5 kpc) and field smc0049, located at an intermediate distance from the SMC center (at ∼3.3 kpc).

Since it is a systematic error, it should be corrected. For such purpose, every solution obtained with this global model CMD should be divided by the solution shown in figure 4 (SMC-mock with 500,000 stars). To test further if such a correction really improves the solutions, we performed a new test, now using a third mock galaxy with a $\psi(t)$ similar to the solutions found for our real SMC fields. The results are shown in figure 6, in which the input $\psi(t)$ for the mock galaxy is represented by the solid line. The recovered SFH for such mock galaxy is represented by the dashed lines in the figure. The recovered $\psi(t)$ differs from the input $\psi(t)$ in the same locations as seen in figure 4: the recovered $\psi(t)$ is higher than the input one at ∼8 Gyr old and lower at ∼10 Gyr old. The obtained $\psi(t)$ (after dividing) is in excellent agreement with the input $\psi(t)$ as seen from the figure (dotted line).

Given that the observational errors differ from field to field, we recovered the systematic signature on the SFH using the SMC-mock SFH for each of the SMC fields, and for the three different sets of age intervals. Then, we divided each SFH we obtained by the corresponding systematic signature.

5. The SFH of the SMC fields

In order to reduce sampling problems associated with age binning, we obtained three different solutions for the SFH, $\psi(t, z)$ (see Aparicio & Hidalgo 2009) of each field, using three different age-binning sets (see table 2). The adopted solution will be the average of the three. As an example, figure 7 shows the three solutions obtained with the BaSTI library for field smc0057 together with the adopted solution, the age-metallicity relation and the observed CMD. The left panel shows the 3D population boxes (Hodge 1989) of the three solutions, where $\psi(t, z)$ is represented as a function of age and metallicity. Here, the volume of each bar over the age-metallicity plane gives the mass that has been transformed into stars within the corresponding age-metallicity interval. The adopted solution (right medium panel) is obtained as a cubic spline fit to the three individual solutions after correcting for the systematic errors discussed above. As in figure 3, error bars (vertical) are only indicative, while the actual dispersion of the three solutions (see Aparicio & Hidalgo 2009) should be considered a more realistic representation of the solution uncertainties. The age-metallicity relations shown in the bottom panel have been obtained as the average metallicity of the stars in each age interval for the three individual solutions.

The solutions obtained using the Padua library are very similar to the ones obtained using the BaSTI library and are not presented in the detail of figure 7. Figures 8 and 9 show a summary of the results obtained for all fields using BaSTI and Padua, respectively. They show, for each field, the spline fit together with the results for the 3 age binning sets. From now on, our discussion of the results will use the results from the BaSTI stellar evolution library. Our conclusions are unchanged if we use instead the results from the Padua library.

5.1. Main characteristics of the $\psi(t)$ solutions for our SMC fields

As seen from figure 8, the eastern fields and the central-most field, smc0057, –located in the south– show a large amount of recent star formation. In particular, the eastern fields show a recent enhancement from ∼2 Gyr ago until the present, while smc0057 shows a recent peak of star formation ∼1 Gyr ago, which seems to be mostly extinguished at the present time. This is in agreement with the characteristics derived for the stellar populations in the Magellanic Bridge (Harris 2007) and in other positions in the wing area of the SMC (see, for example, Irwin et al. 1990; McCumber et al. 2005; Chiosi & Vallenari 2007; among others). These $\psi(t)$ enhancements at young ages in the eastern fields and in smc0057 are not seen in other fields located at similar galactocentric distances. The three eastern fields –the only ones presently forming stars– are located in regions of large amount of HI, unlike the rest of our fields, including smc0057.

A conspicuous intermediate-age enhancement peakes between ∼4 and ∼5 Gyr old in all fields. In addition, there is a small enhancement at ∼2-2.5 Gyr old in the southern and in the western fields. This $\psi(t)$ enhancement is shifted toward younger ages, at ∼1.5-2 Gyr old in the eastern fields. Finally, a $\psi(t)$ enhancement at old ages peaks at ∼10 Gyr old in the eastern and southern fields, which seems to be "split" into two, at ∼8 and ∼12 Gyr old, in the western fields. Note that most of the above features remain unchanged when using the Padua stellar evolution library, as seen in figure 9.

5.2. Global bursts and phase mixing in the SMC

Phase mixing in a galaxy occurs when stars initially close in space –for example stars formed in a star forming region– spread out over time because they have slightly different energies and angular momenta. Stars are said to be fully phase mixed if there is no memory left that they were born close together. The rate at which stars phase mix depends on the gravitational potential, on the initial proximity of the stars, and on their orbits. As a consequence of the latter, perfectly circular orbits will never mix in radius, while perfectly radial orbits never mix in angle.

The presence of the $\psi(t)$ enhancements at ∼4-5 Gyr old in all the SMC fields, together with the large variations found for ages younger than ∼2 Gyr old, would suggest that the phase mixing time in the SMC is of the order of ∼2 Gyr. However, we find also evidences for spatial variations at older ages: the western fields present two $\psi(t)$ enhancements at ∼8 Gyr old and at ∼12 Gyr old, while in the rest of the fields there is a single old enhancement occurring ∼10 Gyr ago. This could imply that stars in the SMC take a Hubble time or more to phase mix. However, solutions are noisier and time resolution is worst for older ages, for which this conclusion must be taken very cautiously until more accurate and precise data, sampling a larger area, are available.

5.3. Spatial distribution of the stellar populations in our SMC fields

One of the most intriguing issues regarding the SMC evolution is the age and distribution of its oldest stars. In order to shed light into this, we calculated the age at the 5th percentile of $\psi(t)$ in each of our SMC fields, i.e., the population age by which 5% of the total stars were formed in each field, which is also presented in figure 10. The 5th percentile age in all fields presents a flat distribution at ∼11.5 Gyr. In fact, the slope of the best-fit line in a least-square fit is 0.064 ± 0.015 (almost negligible). This shows that the age of the old

population in all our SMC fields is essentially the same, independently of the galactocentric distance or the position angle. In addition, we constrain the age of the oldest population to be older than ∼11.5 Gyr old. This is in agreement with the recent age determination of the older and single globular cluster in the SMC, NGC121 (Glatt et al. 2008). Our results are also in good agreement with those of Dolphin et al. (2001) who, for an isolated field, located in the northwestern part of the SMC, found that 14±5% of the star formation took place before 11 Gyr ago.

Another important –and controversial– fact regarding Local Group dwarf galaxies in general and the SMC in particular, is the composition of the outer extended stellar populations. The 95th percentile age for all the SMC fields shows a relatively flat distribution (except for the dichotomy East-West in the central-most fields) while going further away from the SMC center. This points out that, at 4.5 kpc from the SMC center, we did not yet reach a region dominated by an old, Milky Way-like, stellar halo. This is stressed by the fact that the 95th percentile age for our outermost field occured at ∼3 Gyr ago. If we would be in such halo dominated region, the 95th percentile and the 5th percentile age should occur at almost the same time for the outermost fields. Our results are in agreement with Noël & Gallart (2007) who found that up to ∼6.5 kpc from the SMC center, the galaxy is composed by both, intermediate-age and old population. In summary, our results indicate that either an old, Milky Way-like, stellar halo does not exist in the SMC or that if it exists, its contribution to the stellar population is negligible at ∼4.5 kpc from the galactic centre.

5.4. On the possible correlation between the $\psi(t)$ enhancements and the SMC-LMC/SMC-MW pericenter passages

In the pioneering work from Murai & Fujimoto (1980), the authors claimed that the existence of the Magellanic Bridge and the inter-Clouds region are partly explained if the SMC closely approached the LMC around 0.2 Gyr ago. Since then, the orbits of the MCs were studied in detail by many authors, through numerical simulations and proper motion studies (see Gardiner et al. 1994; Bekki & Chiba 2005; Kallivayalil et al. 2006; Besla et al. 2007; among others). All models reproduce a pericenter passage between the MCs around ∼0.2 Gyr ago. Coincidently, enhancements of star formation are found at these ages in both galaxies, particularly in the area in which they are facing each other, i.e., the wing area in the SMC and the West part in the LMC (see, for example, Irwin et al. (1990). Given the low temporal sampling of our SMC SFHs for the youngest ages, we cannot probe if the dichotomy East/Southeast-West actually began ∼0.2 Gyr ago. However, the steep behaviour of the $\psi(t)$ 95th percentile age shown in figure 10 indicates that the dichotomy appeared

at an age smaller than ∼1 Gyr ago. This population younger than 1 Gyr old represents ∼7-12% of the total $\psi(t)$ in the wing area. This does not reflect an exceptional increment in the present star formation as compared with the average $\psi(t)$ but it is very significant in the sense that these eastern fields are the only ones in which star formation is currently going on.

Besides this youngest episode, authors such as Bekki et al. (2004), Bekki & Chiba (2005) and Harris & Zaritsky (2004) have claimed that the episodes of enhancement in the SFH of the SMC could be related with pericenter passages between the SMC and the LMC and/or between the SMC and the Milky Way, while Besla et al. (2007) have concluded that the Magellanic Clouds are likely to be in their first pericenter passage about the Milky Way or on a highly eccentric, bound orbit. To explore this, the $\psi(t)$ enhancements in our SFHs are quantified in figure 11, in which the intensity of each $\psi(t)$ enhancement as a function of radius (11(a)), position angle (11(b)), and age for all the fields are represented, together with the pericenter passages of the SMC with respect to the Milky way or the LMC, as predicted by different authors (see figure caption for details). The intensity of each $\psi(t)$ enhancement is defined as the area under a Gaussian function fitted to the elevation in the spline fit shown in figure 8.

Although unclear, there may be a correlation between the SMC-Milky Way encounters given by Kallivayalil et al. (2006; solid arrows) and the enhancements in $\psi(t)$ we found at ∼2.5 Gyr ago, at ∼4.75 Gyr ago and at ∼8 Gyr ago. In the case of pericenter passages between the LMC and the SMC, there only seems to be a coincidence between the most recent encounter ∼0.2 Gyr ago and the youngest $\psi(t)$ enhancement peaked at these ages in our eastern fields. In the other cases, for the published orbits, we see no clear correlation between the pericenter passages and the observed enhancements in our derived SFHs. All in all, the lack of a clear correlation between the computed passages and SFH could be a support to Besla et al. (2007) results including that indicating that the SMC is in its first pericenter passage about the Milky Way.

5.5. Comparison with other works

Since our eastern and western fields, as well as two of our southern ones, overlap the regions from HZ04, we superimposed our SFHs with the ones they obtained as seen in figure 12. In each case the SFHs found by HZ04 are shown in dashed lines. HZ04 used the starFISH code with the following inputs: a subset of the Padua isochrones for three different metallicities (Z=0.001, Z=0.004, Z=0.008) without interpolation, a power law with Salpeter slope for the IMF, and a 50% binary fraction with secondary masses drawn randomly from

the IMF. We averaged the SFR from HZ04 in the last 0.2 Gyr into only one age bin to fit the age resolution we adopted for the youngest population. We also added up the SFR given by HZ04 for each of their three metallicities. HZ04 cover a larger area in the region of our western fields qj0036 and qj0037, so the solution they give includes both of our fields. We compare the HZ04 solution with ours obtained using the Padua stellar evolution library as input in IAC-star/IAC-pop (shown in § 5). With the exception of field qj0033, there is a general disagreement at intermediate ages in all fields, for which HZ04 find either total or quasi-total quiescence during ∼2 Gyr of the life-time of the galaxy. In the western fields, HZ04 find a peak at around 4.5 Gyr ago which is coincident with the one we find.

In order to understand the disagreement between our SFHs and the ones obtained by HZ04, it should be noted that their photometry is shallower and, therefore, the ability to reliably constrain the intermediate-age to old star formation is reduced. Also, their method to derive the SFH is coarser than the one used in this paper (for example, no interpolation in metallicity is performed and so the simple populations are restricted to the metallicities provided in the stellar evolution set).

Our SFHs solutions for the western fields agree quite well with the SFH presented by Dolphin et al. (2001) (using Girardi et al. 2000 models) for a northwestern field located near NGC121. They find a broadly peaked star formation between 5 and 8 Gyr ago and that the star formation almost stopped around 2 Gyr ago.

The $\psi(t)$ enhancement peaked at ∼4-5 Gyr old is in good agreement with the episodes found by Chiosi & Vallenari (2007) between 3 and 6 Gyr ago for three fields located around the SMC clusters K 29, NGC 290, and NGC 265.

Finally, estimates by Sabbi et al. (2009) are broadly consistent with our results, although we have to wait for the results of the detailed, quantitative analysis of the SFH that these authors are carrying on.

5.6. The Chemical Enrichment History

In the computation of the SFH, IAC-pop also provides the age-metallicity relation, which is plotted in the horizontal plane of figure 7. To more clearly show this metallicity law, we determined the median metallicity of stars formed at each age interval, using the following relation (see § 3):

$$Z(t) = \frac{\sum z_i \psi_i(t)}{\sum \psi_i(t)} \tag{3}$$

We adopted $Z_{\odot}$=0.02 in order to convert from Z metallicities to [Fe/H] values and assuming [Fe/H]=log($Z/Z_{\odot}$). The age-metallicity relation computed in this way for the eastern, western, and southern fields are shown with solid line in figure 13 together with the age-metallicity relation found by Carrera et al. (2008b) (see their table 6) using Ca II triplet spectroscopy of RGB stars from the same fields analysed in this paper. The $\pm 1 sigma$ dispersion of the stellar metallicity distribution as a function of age as derived in this paper, and the metallicity dispersion of the Ca II triplet metallicities in each bin, from Carrera (2008b) have also been represented.

The age-metallicity relations in all fields (13(a), 13(b), 13(c)) show a continuously increasing metallicity from an early epoch until now. For the southern fields, there is an excellent agreement with the findings of Carrera et al. (2008b). The agreement is good in the case of the eastern and western fields, with small differences for ages older than 5 Gyr, for which we find a lower metallicity in the west and a higher metallicity in the east than those of Carrera et al. (2008b). These results, taken together, are an important test of IAC-pop because they show, for the first time, the external consistency of the code in determining the chemical enrichment law.

Tsujimoto & Bekki (2009) claim that a dip is detected in the [Fe/H]-age relation in the SMC and that would be related to a major merging event occurred some 7.5 Gyr ago. We have to mention that such dipping is not visible in the age-metallicity relations derived in our analysis.

6. Discussion and Conclusions

We have presented a detailed study of the SFH of 12 fields located in the Small Magellanic Cloud, based on a set of [*(B-R), R*] CMDs that reach the oldest MS turnoffs ($M_R \sim 3.5$). The spatial distribution of the fields, located at different galactocentric distances and azimuths, makes it possible to distinguish the stellar content in the wing area and in the "undisturbed" parts toward the western and southern regions of the SMC (see figure 1), and to study possible stellar population variations with galactocentric radius. We used the IAC-star and IAC-pop codes to obtain the SFH, $\psi(t, z)$. The results of this analysis allow us to accurately constrain the parameter space defining the SFHs of the 12 SMC fields. The fact that the main characteristics of $\psi(t, z)$ are unchanged for different combinations of parameters, including different stellar evolution libraries, indicates that our solutions for the SFHs are robust. In addition, common patterns, which vary smootly with position, appear in most fields. As final inputs for IAC-star/IAC-pop we used the BaSTI (Pietrinferni et al. 2004) and Padua (Bertelli et al. 1994) stellar evolution libraries, the bolometric corrections

from Castelli & Kurucz (2003), the Kroupa's revised IMF (Kroupa et al. 2003), and a 30% of binaries with a mass ratio $q \gtrsim 0.7$. All the $\psi(t,z)$ solutions have $\chi^2_{\nu,min} < 2$.

In the retrieved SFHs of our SMC fields, we found the following. There are four main episodes of enhancement in $\psi(t)$: one at young ages, only present in the eastern fields (the ones facing the LMC) and in the central-most one (located in the south), peaked at ∼0.2-0.5 Gyr ago; two at intermediate ages, a conspicuous one peaked at ∼4-5 Gyr old in all fields and a less significant one peaked at ∼1.5-2.5 Gyr old in all fields; and one at old ages, with the peak at ∼10 Gyr old in all fields but the western ones, in which this old enhancement is split into two at ∼8 Gyr old and at ∼12 Gyr old. There are smaller enhancements and variations from field to field that are less significant.

The fact that all fields present $\psi(t)$ enhancements at ∼1.5-2.5 Gyr old and at ∼4-5 Gyr old could mean that, at these ages, there were global episodes of star formation in the SMC. Alternatively, these episodes could have been produced in a particular region of the SMC and then the stars could have spread all over the galaxy, such that stars older than ∼1.5-2.5 Gyr old are well mixed, both in radius and in azimuth. The large variations for ages younger than ∼1.5-2.5 Gyr old and the common burst of ∼1.5-2.5 Gyr old would suggest that the phase mixing time in the SMC is of the order of ∼1.5 Gyr. However, we find also evidence for variations at old ages (a $\psi(t)$ enhancement at 10 Gyr old in the East and in the South but at ∼8 and ∼12 Gyr old in the western fields). These differences at old ages seem to be robust features. If so, they could imply that stars in the SMC take a Hubble time or more to phase mix. Alternatively, they could be the result of recently dissolved old star/globular clusters. In future work, it will be interesting to determine the SFHs over larger areas at different azimuths in order to confirm the dichotomy in the SFH at old ages and to constrain the spatial limits of this "two-enhancements zone". This, with the aid of theoretical models, will help to address the possible origin of such enhancements in $\psi(t)$.

The eastern fields are located in a region of high HI concentration (see figure 8). We found that the young population present in this wing area in the last 1 Gyr represents between ∼7-12% of the total stars found in it. This indicates that, although the young population does not reflect an exceptional increase of the star formation at the present time with respect to the average $\psi(t)$, this increase is important in global terms since this wing area is the only part of our study in which there is active and conspicuous star formation presently going on[6].

The young $\psi(t)$ enhancement may have been triggered by a close encounter between the

[6]It is worth noticing that the highest current star formation activity is in the central, bar region of the galaxy, which is not studied here. In such area, several strong HII regions are located.

SMC and the LMC at these ages, as indicated by studies of the MCs orbits, both from numerical simulations and proper motions (Murai & Fujimoto 1980; Gardiner et al. 1994; Bekki & Chiba 2005; Kallivayalil et al. 2006; among others). Given the low temporal resolution of our SMC SFHs for young ages, we cannot probe if the dichotomy East/Southeast-West actually began ∼0.2 Gyr ago. However, the step behaviour of the $\psi(t)$ 95th percentile age shown in figure 10 indicates that the dichotomy appeared at an age smaller than ∼1 Gyr ago.

A correlation may exists between past $\psi(t)$ enhancements and the perigalactic encounters between the SMC and the Milky Way for the orbits given by Kallivayalil et al. (2006). But this correlation is unclear and there is nothing against the Magellanic Clouds being in their first perigalactic passage as claimed by Besla et al. (2007). On another side, with the exception of the $\psi(t)$ enhancement peaked ∼0.2 Gyr ago in the Eastern fields, we do not find a clear correlation between the enhancements in $\psi(t)$ and the pericenter passages between the SMC and the LMC as computed by Bekki & Chiba (2005) and by Kallivayalil et al. (2006).

The flat distribution at ∼12 Gyr old of the age at the 5th percentile indicates that the age of the oldest population is remarkably similar in all fields at all radii and at all azimuths and constrains the age of the oldest stars in our SMC fields to be older than 12 Gyr old. This is also seen in other Local Group galaxies, such as Phoenix, a smaller and non-interacting galaxy (see Hidalgo et al. 2009).

We did not reach a region dominated by an old, Milky Way-like, stellar halo at 4.5 kpc from the SMC center. This indicates that either an old, Milky Way-like, stellar halo does not exist in the SMC or that if it exists, its contribution to the stellar population is negligible at ∼4.5 kpc. These results are in agreement with Noël & Gallart (2007) who found no signs of an old stellar component domination at ∼6.5 kpc from the SMC center.

Finally, from our SFH solutions, we also retrieved a chemical enrichment history for our SMC fields. On average, all fields show a continuously increasing chemical enrichment from an early epoch until now. Our derived age-metallicity relations are in good agreement with the findings of Carrera et al. (2008b) using the CaII triplet. This is external consistency proof of IAC-pop in determining the chemical enrichment law.

We are very grateful to Mike Beasley, Ricardo Carrera, Santi Cassisi, Gary Da Costa, Ken Freeman and Matteo Monelli for interesting comments and illuminating discussions. We also thank Justin I. Read for many very useful comments and discussions which improved this manuscript in its early stages. This work has been founded by the Instituto de Astrofísica de Canarias (P3-94) and by the Ministry of Education and Research of the Kingdom of Spain

(AYA2004-06343 and AYA2007-67913). E. C. and R. A. M. acknowledge support by the Fondo Nacional de Investigación Científica y Tecnológica (No. 1050718, Fondecyt) and by the Chilean Centro de Astrofísica FONDAP (No. 15010003). This project has made generous use of the 10% Chilean time, and continuous support from the CNTAC and Las Campanas staff is greatly appreciated. N.E.D.N. acknowledges the hospitality of the astrophysics group at Zürich University.

Table 1. Reddening values

Field	E(B-V)
smc0057	0.09
qj0037	0.07
qj0036	0.07
qj0111	0.09
qj0112	0.09
qj0116	0.08
smc0100	0.05
qj0047	0.05
qj0033	0.03
smc0049	0.06
qj0102	0.05
smc0053	0.06

Table 2. Age intervals

name	age intervals (in Gyr)
age-1	0 0.5 1 2 3 4 5 7 9 11 13
age-2	0 0.2 0.5 1.1 1.8 2.7 3.9 5.4 7.2 9 11 13
age-3	0 0.1 0.2 0.5 1 1.9 2.7 3.3 4.1 5 6 7.1 9 10.7 13

Table 3. Metallicity intervals

name	metallicity intervals
metal-1	0.0001 0.0003 0.0006 0.001 0.0015 0.002 0.003 0.004 0.005 0.006 0.008 0.01 0.015 0.02
metal-2	0.0001 0.0003 0.0006 0.001 0.0015 0.002 0.003 0.004 0.006 0.008

Table 4. Age-metallicity pairs

Simple populations	age intervals	metallicity intervals	fields
90	10	9	qj0047, smc0049, qj0102, smc0053, qj0033, qj0036, qj0037
99	11	9	qj0047, smc0049, qj0102, smc0053, qj0033, qj0036, qj0037
126	14	9	qj0047, smc0049, qj0102, smc0053, qj0033, qj0036, qj0037
130	10	13	smc0057, smc0100, qj0111, qj0112, qj0116
143	11	13	smc0057, smc0100, qj0111, qj0112, qj0116
182	14	13	smc0057, smc0100, qj0111, qj0112, qj0116

Table 5. $\chi^2_{\nu,min}$ for the solutions $\psi(t,z)$ in the SMC fields

field	$\chi^2_{\nu,min}$ age-1	$\chi^2_{\nu,min}$ age-2	$\chi^2_{\nu,min}$ age-3
smc0057	1.19	1.36	1.46
qj0037	1.12	1.13	1.26
qj0036	1.13	1.21	1.26
qj0111	1.43	1.45	1.62
qj0112	1.41	1.47	1.57
qj0116	1.45	1.57	1.58
smc0100	1.58	1.78	1.53
qj0047	1.64	1.74	1.78
qj0033	0.88	0.93	0.92
smc0049	1.38	1.55	1.41
qj0102	1.33	1.47	1.31
smc0053	1.21	1.27	1.39

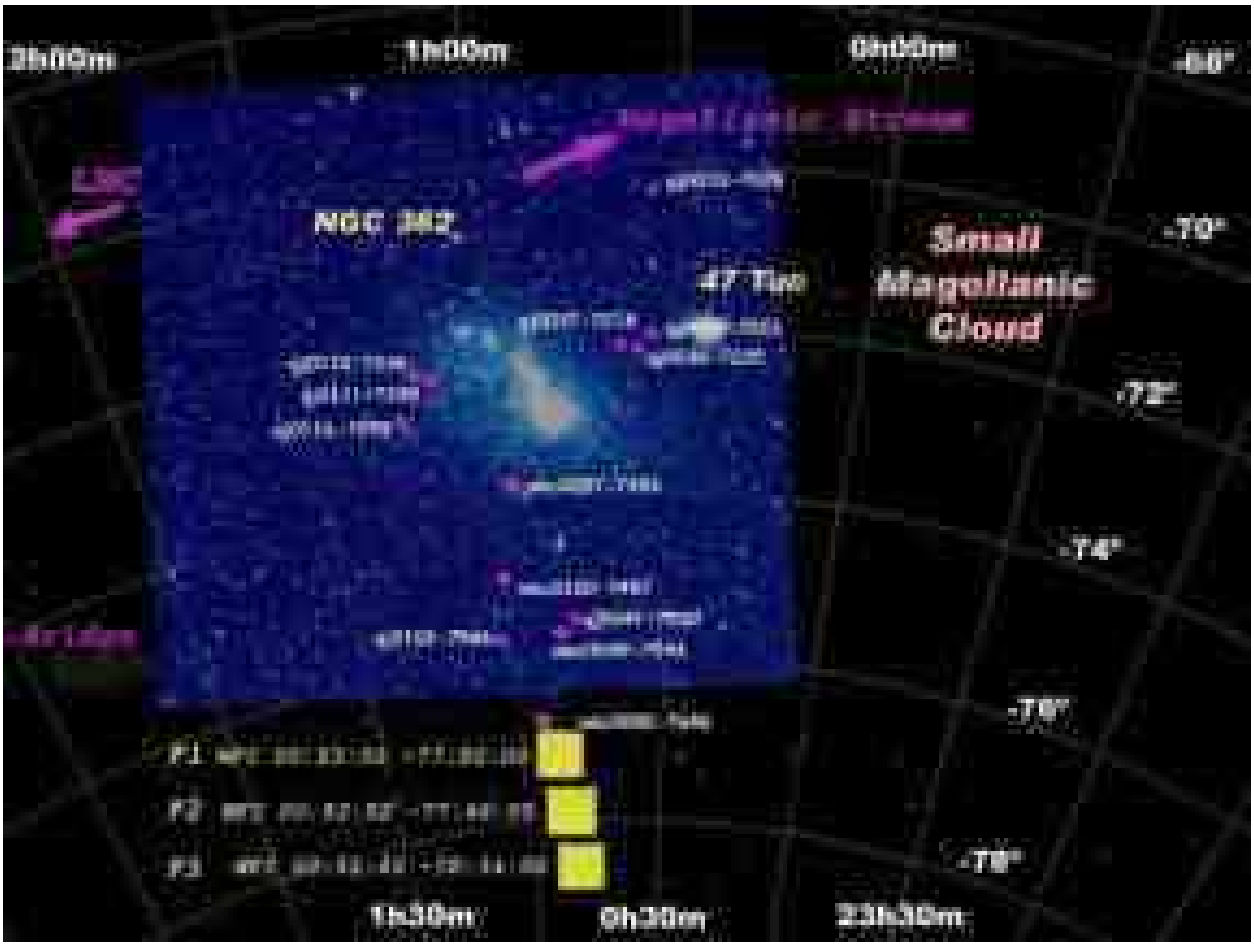

Fig. 1.— Spatial distribution of our SMC fields. The large squares denote the $34' \times 33'$ fields analyzed in Noël & Gallart (2007). The small symbols represent the fields analyzed here and in Paper I.

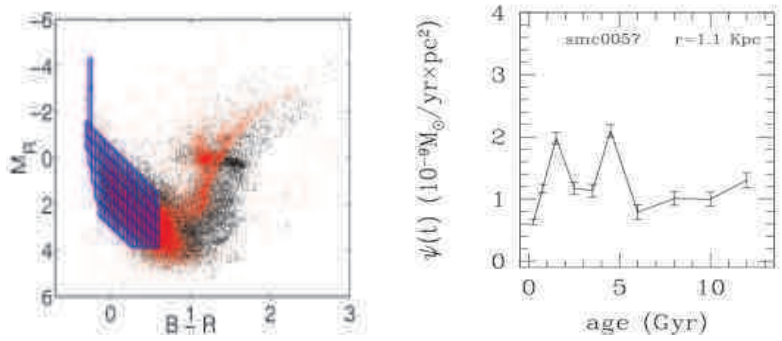

(a) "*à la carte*" parameterization (b) Solution with $\chi^2_{\nu,min}$=1.21

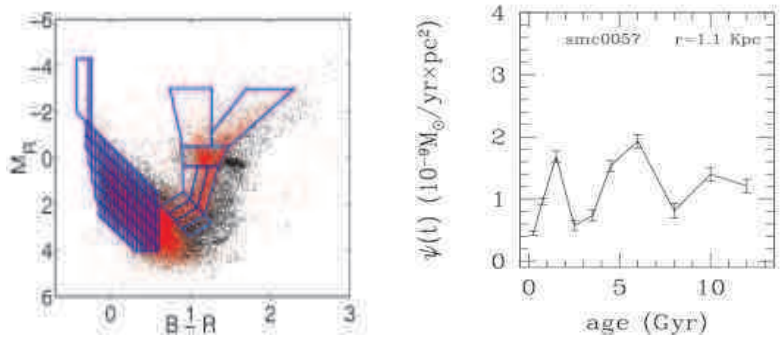

(c) "*à la carte*" parameterization (d) Solution with $\chi^2_{\nu,min}$=1.49

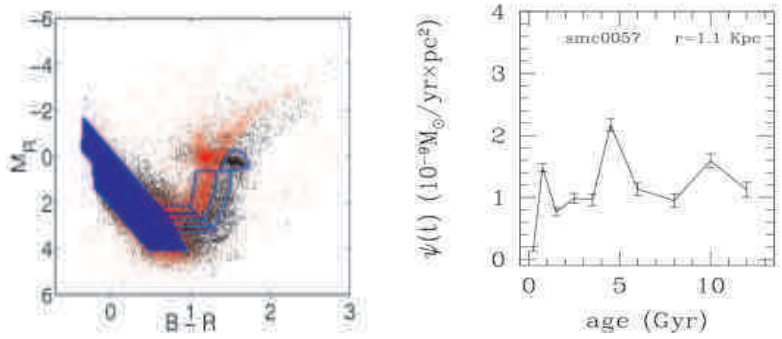

(e) "*à la carte*" parameterization (f) Solution with $\chi^2_{\nu,min}$=1.96

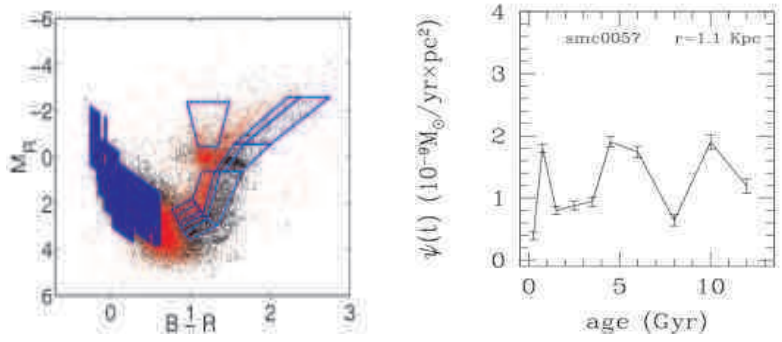

(g) '*à la carte*" parameterization (h) Solution with $\chi^2_{\nu,min}$=2.01

Fig. 2.— Left panels show some examples of the parameterizations we performed on the observed (red) and model (black) CMDs using BaSTI library. The corresponding solutions are shown in the panels on the right. Error bars have been computed as the dispersion of 20

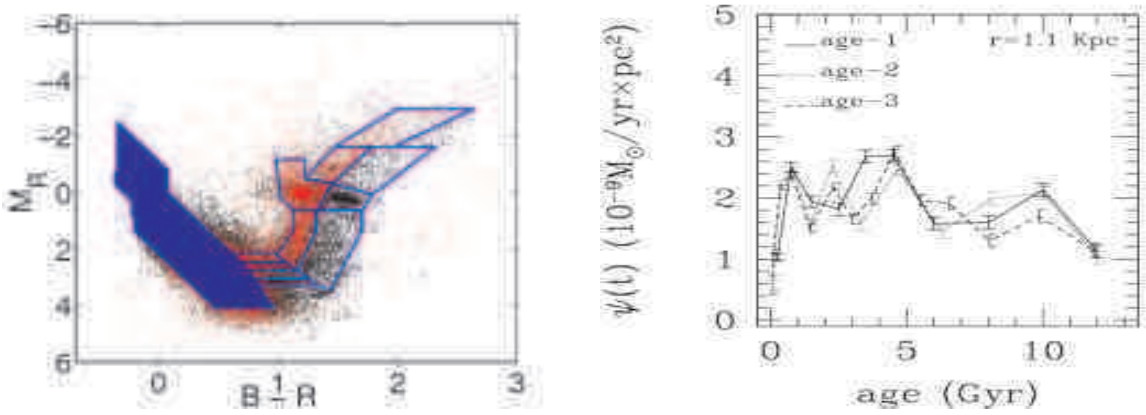

(a) Using "*à la carte*" parameterization

(b) Using "*à la carte*" parameterization

Fig. 3.— Panel 3(a) shows the final set of boxes used to obtain the $\psi(t, z)$ of our SMC fields. For the MS, we used a *quasi*-grid parameterization. We follow the isochrone's track as a guide and for the subgiant branch, the RGB and the RC larger boxes were carefully selected in order to avoid introducing errors. The final solution is shown in 3(b) for three different age binnings.

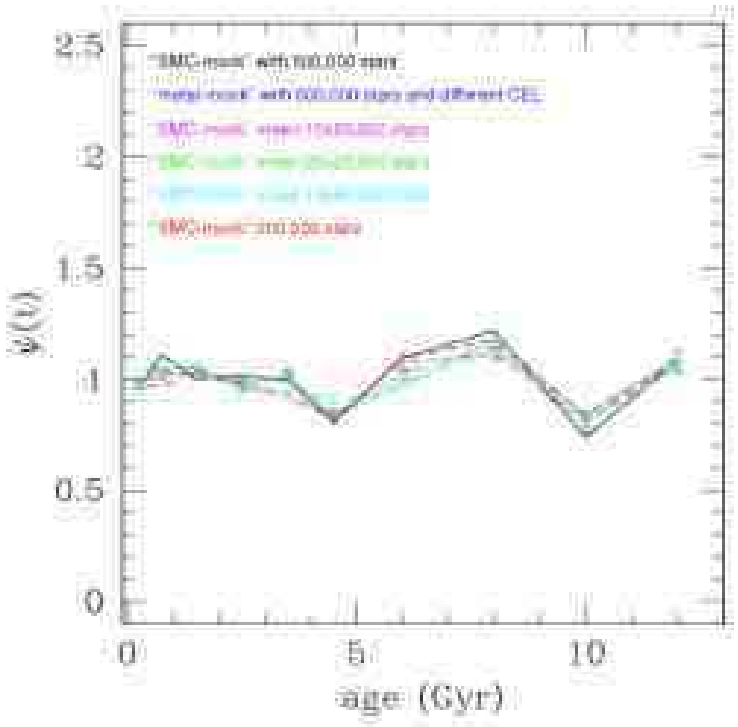

Fig. 4.— The solution for the SFH of several samples of the "SMC-mock" and "metal-mock" synthetic populations are shown. The input $\psi(t)$=1 and the input metallicity law is one suitable for the SMC. In the case of the mean SFHs the errors are defined as: $\sigma/(\text{N-1})^{1/2}$, where σ^2 is the variance. There is a systematic deviation from the input ($\psi(t)$=1) SFH, showing "wiggles". See text for details.

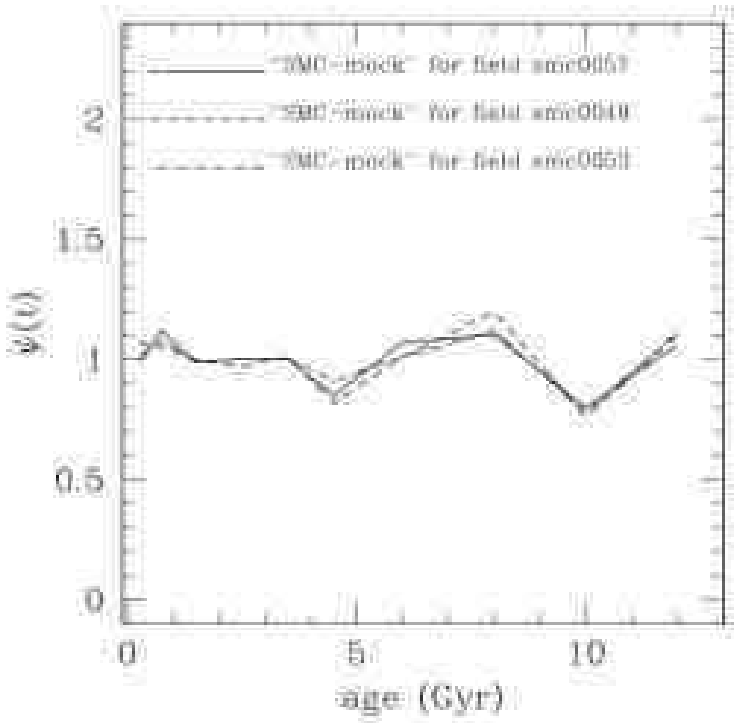

Fig. 5.— SMC-mock SFHs obtained simulating the observational errors for three SMC fields located at different galactocentric distances: smc0057 (at ∼1.1 kpc), smc0049 (at ∼3.3 kpc), and smc0053 (at ∼4.5 kpc).

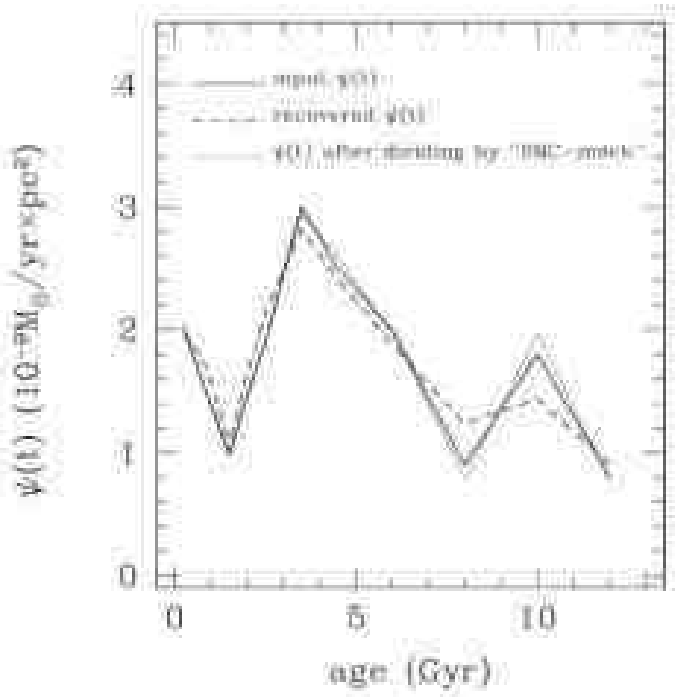

Fig. 6.— Input, recovered, and solution $\psi(t)$ for a given galaxy with similar characteristics to the $\psi(t)$ obtained for the SMC fields. Given the input $\psi(t)$, the recovered $\psi(t)$ slightly differs in the age bins seen in figure 4. It is clear that the final $\psi(t)$, obtained after dividing the input $\psi(t)$ by the "SMC-mock" with 500,000 stars, is in excellent agreement with the input $\psi(t)$.

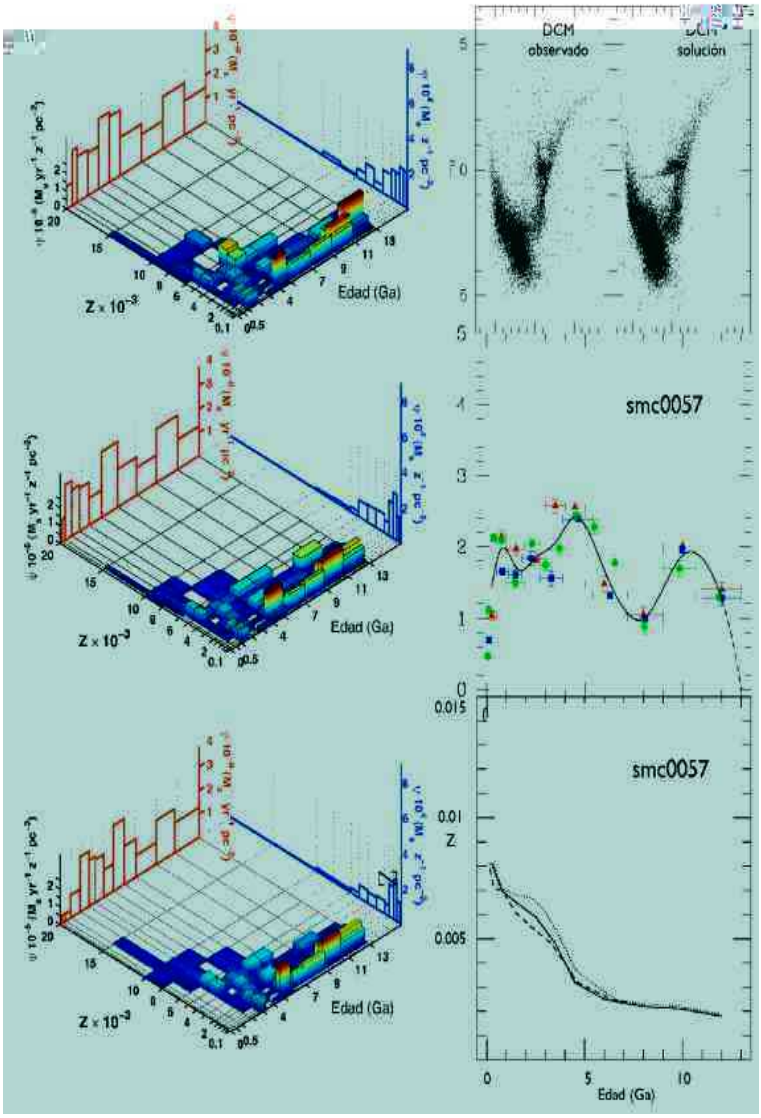

(a) Field smc0057

Fig. 7.— Left panel: three-dimensional representation of the solution for the SFH of the labelled field. The x-axis shows the age of the stars (in Gyr), the y-axis shows the metallicity of the stars, and the z-axis shows $\psi(t)$, in units of solar masses per year, metallicity interval, and area. $\psi(t, z)$ in each age-interval is given by the height of the bar emerging from the xy plane. Right panel: observed and solution CMDs (above), $\psi(t)$ solutions for the three age binnings (middle) and corresponding age-metallicity relations (bottom). Each of the individual $\psi(t)$ solutions were corrected by the systematic errors discussed in Sec. 4.1 and are represented by a different symbol and color: red triangles are for age-1, blue squares are for age-2, and green circles are for age-3. Each $\psi(t)$ point carries its vertical error bar that is the formal error from IAC-pop, calculated as the dispersion of 20 solutions with χ^2_ν=$\chi^2_{\nu,min}$+1, where $\chi^2_{\nu,min}$ is that of the solution shown in the figure (see Aparicio & Hidalgo 2009). Horizontal tracks are not error bars but show the age interval associated to each point. The results for the three age-binning sets were combined by fitting a cubic spline. We do not have a constraint on $\psi(t)$ at 13 Gyr old and so the end point of our spline fit is arbitrary.

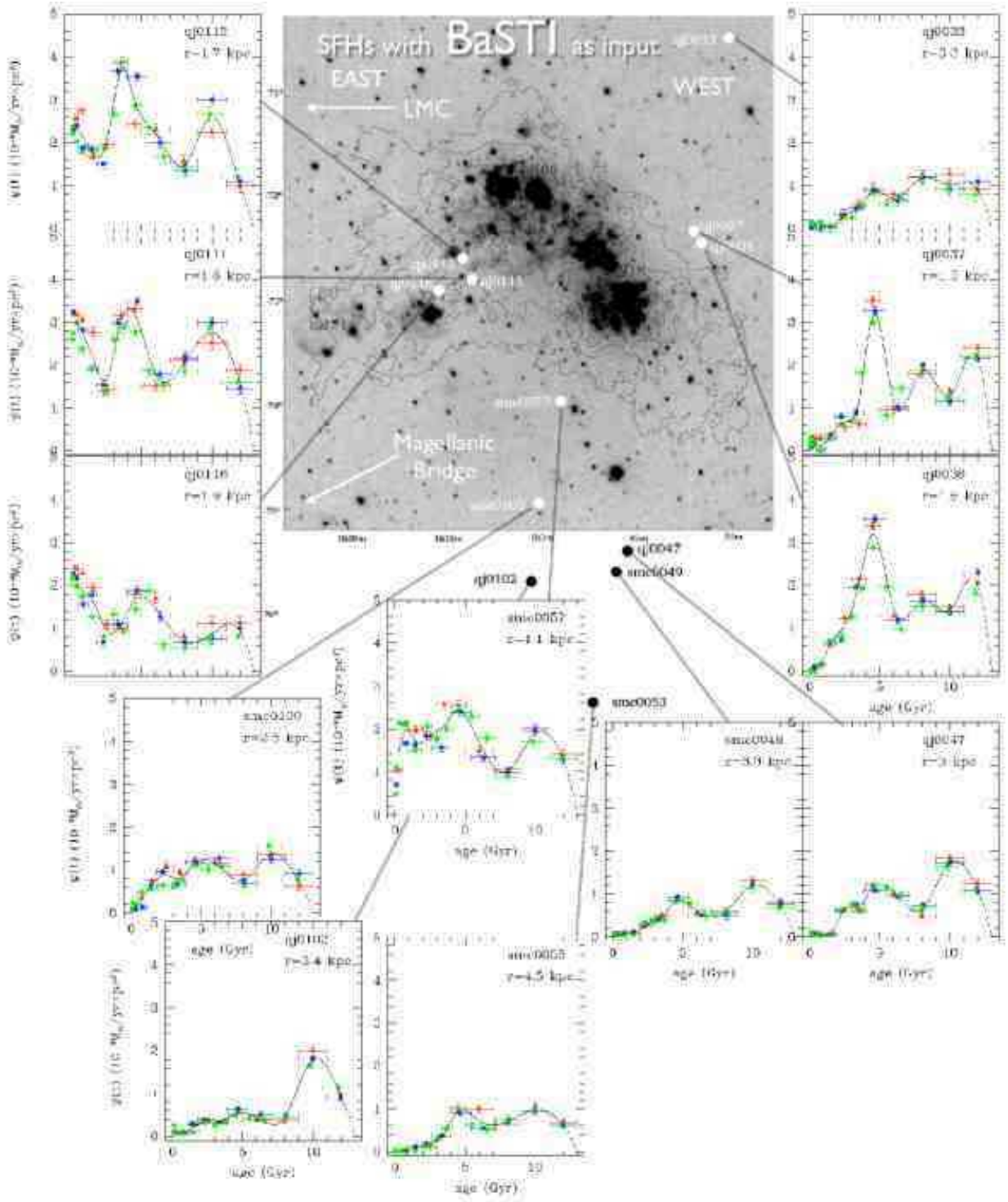

Fig. 8.— The derived SFHs of our SMC fields. BaSTI stellar evolution library was used as input of IAC-star. Each solution shows the SFH obtained for 3 three age binning schemes from table 2 (red triangles: age-1, blue squares age-2, and green circles age-3). Each point carries its vertical error bar that is the formal error from IAC-pop, calculated as the dispersion of 20 solutions with χ^2_ν=$\chi^2_{\nu,min}$+1. Horizontal tracks are not error bars, but show the age interval associated to each point. The solid line shows the results of a cubic spline fit to the results. We do not have a constraint on the $\psi(t)$ at 13 Gyr old and the end point of our spline fit was chosen to be zero arbitrarily (dashed lines between 12 and 13 Gyr age in the

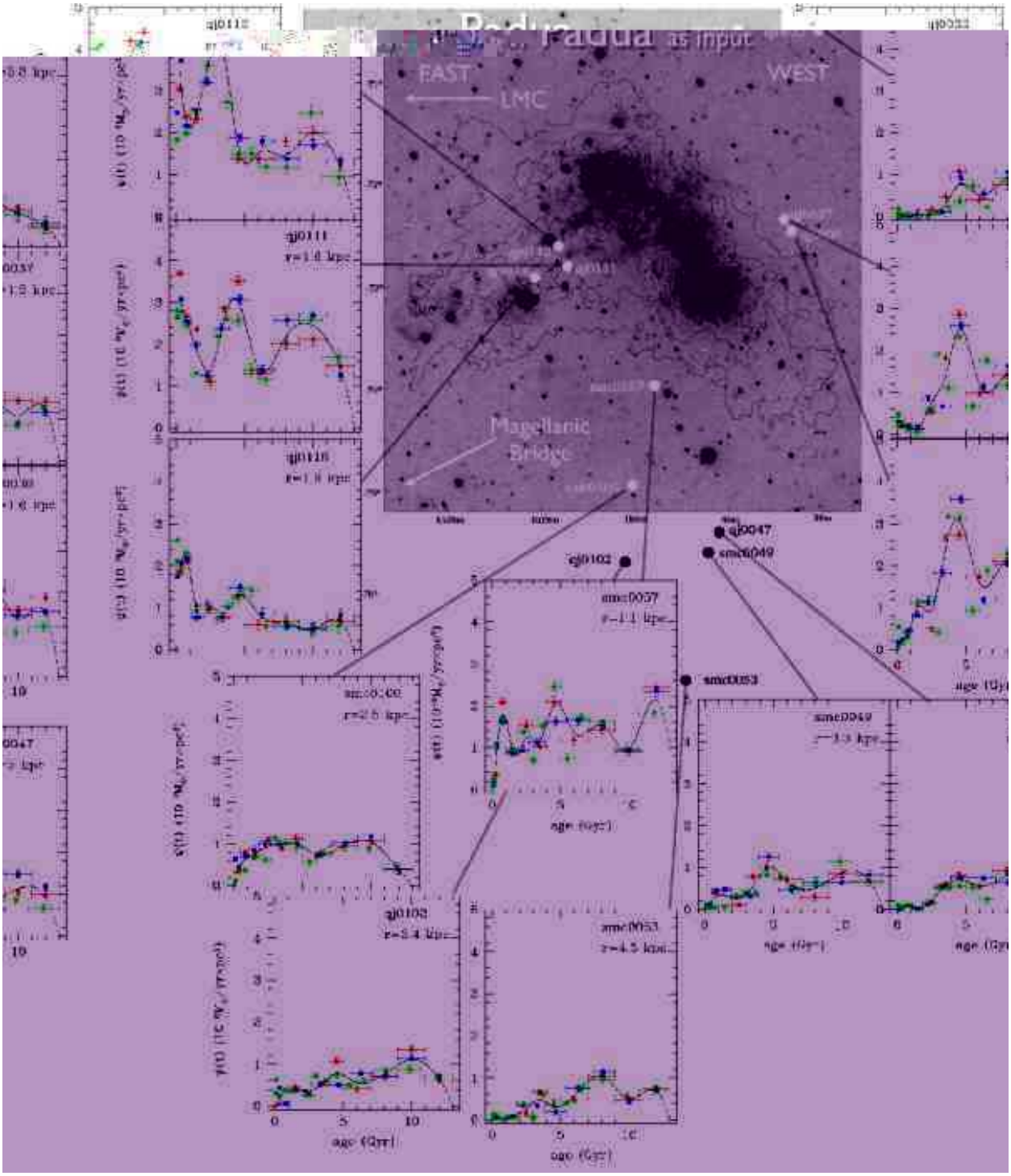

Fig. 9.— Same as figure 8 but using Padua stellar evolution library as input of IAC-star. Note that the main characteristics seen in figure 8 are impervious to the change of stellar evolution library.

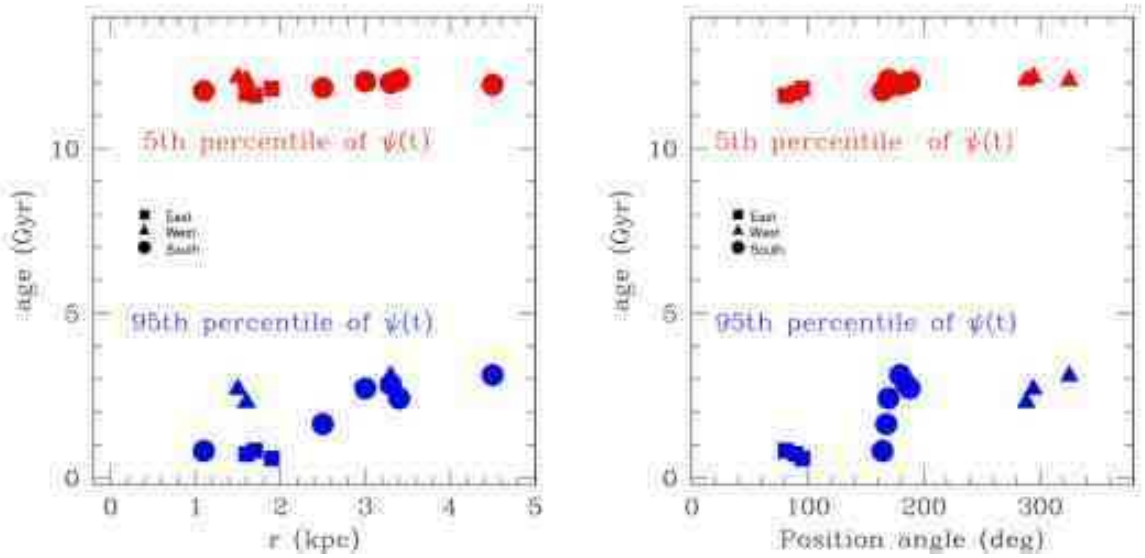

(a) age vs radius

(b) age vs position angle

Fig. 10.— The age at the 5th and at the 95th percentiles of $\psi(t)$ for each of our SMC fields are represented as a function of radius, position angle, and age. See text for details.

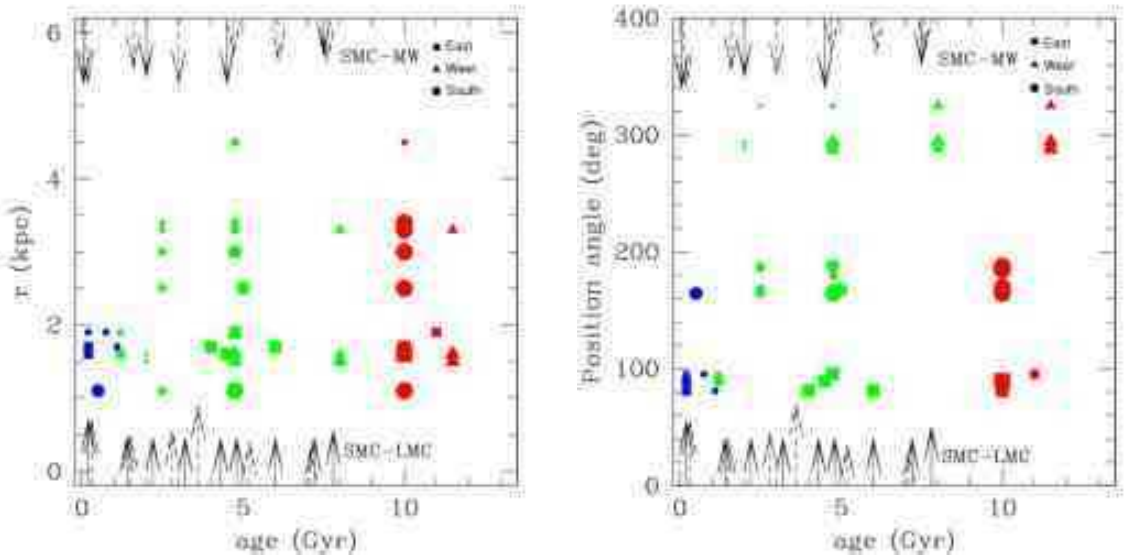

(a) Intensity of $\psi(t)$ enhancements (age vs. radius). (b) Intensity of $\psi(t)$ enhancements (age vs. position angle).

Fig. 11.— Intensity of the $\psi(t)$ enhancements together with pericenter passages of the SMC. We fitted a gaussian function to the elevations in figure 8. The size of the symbols depends on the intensity of the enhancement. The bottom arrows indicate the pericenter passages with the LMC while the top arrows show the encounters with the Milky Way (solid-lined arrow represent data from Kallivayalil et al. 2006 and dashed-lined ones are data obtained from Bekki & Chiba 2005). The size of the arrows represent the intensity of the encounter. Note that some enhancements are hidden behind larger ones. See text for details.

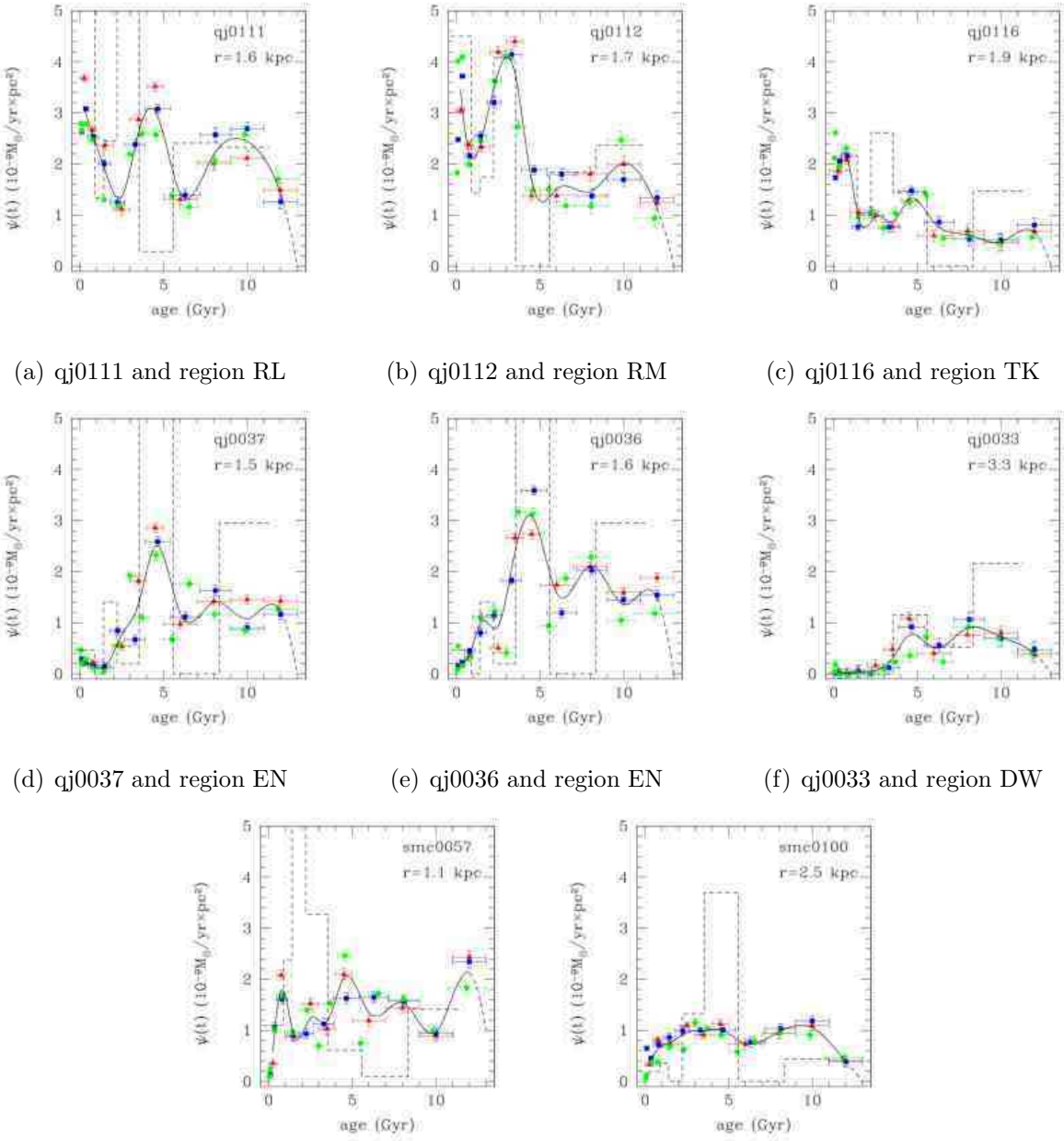

(a) qj0111 and region RL (b) qj0112 and region RM (c) qj0116 and region TK

(d) qj0037 and region EN (e) qj0036 and region EN (f) qj0033 and region DW

(g) smc0057 and region MF (h) smc0100 and region NA

Fig. 12.— Comparison of the SFHs obtained in this work using the Padua stellar evolution library as input in IAC-star (see figure 9) and the ones obtained by HZ04 (dashed lines) for the overlapping fields. Their EN region covers a larger area, including both fields qj0036 and qj0037. See text for details.

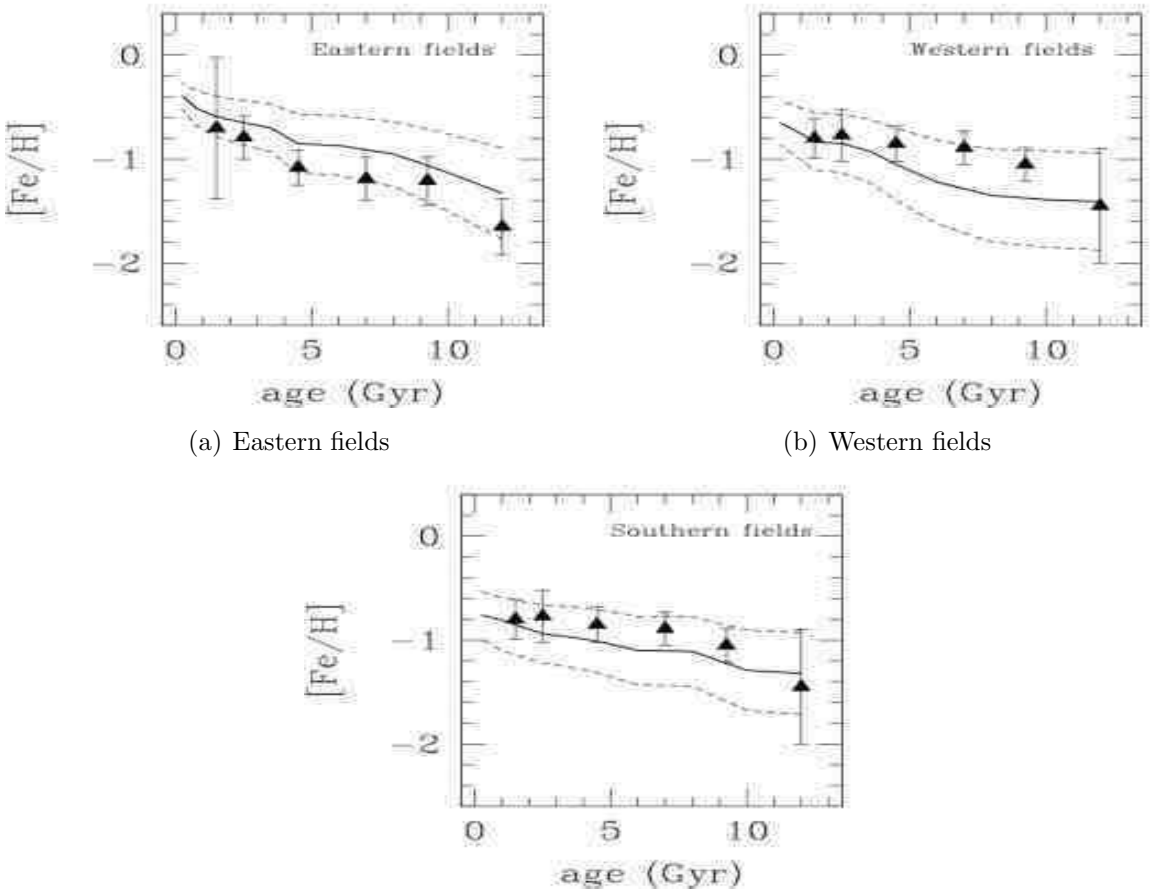

(a) Eastern fields

(b) Western fields

(c) Southern fields

Fig. 13.— The averaged age-metallicity relations ([Fe/H] as a function of age) for the eastern, western, and southern fields are shown with a solid line. The dotted lines represent the $\pm 1\sigma$ level. The triangles represent the age-metallicity relations found by Carrera et al. (2008b) (see their table 6).

REFERENCES

Alcock, C., Allsman, R. A., Alves, D. R., Axelrod, T. S., Becker, A. C., Bennett, D. P., Bersier, D. F., Cook, K. H., Freeman, K. C., Griest, K., y 13 coauthors 1999, AJ, 117, 920

Aparicio, A., & Gallart, C. 1995, AJ, 110, 2105

Aparicio, A., & Gallart, C. 2004, AJ, 128, 1465

Aparicio, A., & Hidalgo, S.L. 2009, accepted

Bekki, K., & Chiba, M. 2005, ApJ, 625, 107L

Bekki, K., Couch, W. J., Beasley, M. A., Forbes, D. A., Chiba, M., Da Costa, G. S. 2004, ApJ, 610, 93L

Bertelli, G., Bressan, A., Chiosi, C., Fagotto, F., & Nasi, E. 1994, A&AS, 106, 275

Besla, G., Kallivayalil, N., Hernquist, L., Robertson, B., Cox, T. J., van der Marel, R., & Alcock, C. 2007, ApJ, 668, 949

Bica, E., Bonatto, C., Dutra, C.M., & Santos, J.F.C., Jr. 2008, MNRAS, 389, 678

Carlson, L. R., Sabbi, E., Sirianni, M., and 9 coauthors 2007, ApJ, 665, 109L

Carrera, R., Gallart, C., Aparicio, A., Costa, E., Méndez, R. A., & Noël, N. E. D. 2008b, AJ, 136, 1039

Carrera, R., Gallart, C., Hardy, E., Aparicio, A., & Zinn, R. 2008a, AJ, 135, 836

Carretta, E., Gratton, R. G., Clementini, G., & Fusi Pecci, F. 2000, ApJ, 533, 215

Castellani V., Degl'Innocenti S., Marconi M., Prada Moroni P. G., Sestito P. 2003. A&A, 404, 645

Castelli, F. & Kurucz, R.L. 2003, in Modelling of Stellar Atmospheres, IAU Symp., 210, 20

Chiosi, E., Vallenari, A., Held, E.V., Rizzi, L. & Moretti, A. 2006, å, 452, 179

Chiosi, E. & Vallenari, A. 2007, å, 466, 165

Cioni, M.-R. L., Habing, H. J., & Israel, F. P. 2000, A&A, 358, 9L

Cioni, M.-R. L., Girardi, L., Marigo, P., & Habing, H. J. 2006, A&A, 452, 195

Cordier, D., Pietrinferni, A., Cassisi, S., Salaris, M. 2007, AJ, 133, 468

Costa, E., Méndez, R. A., Pedreros, M., Moyano, M., Gallart, C., Noël, N. E. D., Baume, G., & Carraro, G. 2009 , AJ, 137, 4339

de Vaucouleurs G., de Vaucouleurs A., Corwin H. G., Buta R. J., Paturel G., Fouque P., 1991, Third Reference Catalogue of Bright Galaxies. Springer, Berlin

Dolphin, A. E., Walker, A. R., Hodge, P. W., Mateo, M., Olszewski, E. W., Schommer, R. A., & Suntzeff, N. B. 2001, ApJ, 562, 303

Dufour, R. J. 1975, ApJ, 195, 315

Dufour, R. J. 1984, in Structure and Evolution of the Magellanic Clouds, IAU Symp., 108, 353

Dufour, R. J., & Harlow, W. V. 1977, ApJ, 216,706

Gallart, C., Freedman, W. L., Aparicio, A., Bertelli, G. 1999, AJ, 118, 2245

Gallart, C., Zoccali, M., & Aparicio, A. 2005 ARA&A, 43, 10

Gardiner, L. T., & Hatzidimitriou, D. 1992, MNRAS, 257, 195

Gardiner, L. T., Sawa, T., & Fujimoto, M. 1994, MNRAS, 266, 567

Girardi, L., Bressan, A., Bertelli, G., Chiosi, C. 2000, A&AS, 141, 371

Glatt, K., Gallagher, J. S. III., Grebel, E. K., and 8 coauthors 2008a, AJ, 135, 1106

Glatt, K., et al. 2008b, AJ, 135, 1106

Harris, J. 2007, ApJ, 658, 345

Harris, J., & Zaritsky, D. 2001, ApJS, 136, 25

Harris, J., & Zaritsky, D. 2004, AJ, 127, 1531 (HZ04)

Harris, J., & Zaritsky, D. 2006, AJ, 131, 2514

Hatzidimitriou, D., Croke, B. F., Morgan, D. H., & Cannon, R. D. 1997, A&AS, 122, 507

Henize, K. G. 1956, ApJS, 2, 315

Hidalgo, S. L., Aparicio, A., & Martínez-Delgado, D. 2003, Ap&SS, 284, 595

Hidalgo, S. L., Aparicio, A., & Martínez-Delgado, D., 2008, submitted to AJ.

Hilditch, R. W., Howarth, I. D., & Harries, T. J 2005, MNRAS, 357, 304

Hunter, D. A., & Elmegreen, B. G. 2004, AJ, 128, 2170

Irwin, M. J., Demers, S., & Kunkel, W. E. 1990, AJ, 99, 191

Kallivayalil, N., van der Marel, R. P., & Alcock, C. 2006, ApJ, 652, 1213

Keller, S. C., & Wood, P. R. 2006, ApJ, 642, 834

Kleyna, J.T., Wilkinson, M.I., Evans, N.W., Gilmore, G. 2001, ApJ, 563, 115L

Komiyama, Y., Doi, M., Furusawa, H., Hamabe, M., Imi, K., Kimura, M., Miyazaki, S., Nakata, F., Okada, N., Okamura, S., and 5 coauthors 2007, AJ, 134, 835

Kroupa, P. Bouvier, J., Duchne, G., Moraux, E. 2003, MNRAS, 346, 354

Maragoudaki, F., Kontizas, M., Morgan, D. H., Kontizas, E., Dapergolas, A., & Livanou, E. 2001, A&A, 379, 864

Massey, P. 2002, ApJS, 141, 81

Mathewson, D. S., Ford, V. L., & Visvanathan, N. 1988, ApJ, 333, 617

McCumber, M. P., Garnett, D. R., & Dufour, R. J. 2005, AJ, 130, 1083

Mighell, K. J. 1999, ApJ, 518, 380

Murai T., & Fujimoto M. 1980, PASJ, 32, 581

Noël, N. E. D., Gallart, C., Costa, E., & Méndez, R.A. 2007, AJ, 133, 2037 (Paper I)

Noël, N. E. D., & Gallart, C. 2007, ApJ, 665, 23L

Peimbert, M., Peimbert, A., & Ruiz, M. T. 2000. ApJ, 541, 688

Peimbert, M., & Torres-Peimbert, S. 1976, ApJ, 203, 581

Piatek, S., Pryor, C., & Olszewski, E. W. 2008, AJ, 135, 1024

Piatti, A.E., Geisler, D., Sarajedini, A., Gallart, C., Wischnjewsky, M. 2008, MNRAS, 389, 429

Pietrinferni, A., Cassisi, S., Salaris, M. & Castelli, F. 2004, ApJ, 612, 168

Pietrinferni, A., Cassisi, S., Salaris, M. & Castelli, F. 2006, ApJ, 642, 797

Rafelski, M., & Zaritsky, D. 2005, AJ, 129, 2701

Schaller G., Schaerer D., Meynet G., & Maeder A. 1992, A&AS, 96, 269

Spergel, D. N., Verde, L., Peiris, H. V., Komatsu, E., Nolta, M. R., Bennett, C. L., Halpern, M., Hinshaw, G., Jarosik, N., Kogut, A., Limon, M., Meyer, S. S., Page, L., Tucker, G. S., Weiland, J. L., Wollack, E., & Wright, E. L. 2003, ApJS, 148, 175

Stetson, P. B. 1994, PASP, 106, 250

Storm, J., Carney. B. W., Gieren, W. P., Fouqué, P., Latham, D. W., & Fry, A. M. 2004, A&A 415, 531

Stanimirovič, S., Staveley-Smith, L., Dickey, J. M., Sault, R. J. & Snowden, S. L. 1999, MNRAS, 302, 417

van den Bergh, S. 1999, A&AR, 9, 273

Walker, M. G., Mateo, M., Olszewski, E.W., Pal, J.K., Sen, B., Woodroofe, M. 2006, ApJ, 642, 41L

Westerlund, B. E. 1997, The Magellanic Clouds (Cambridge: Cambridge Univ. Press)

Wilke, K., Klaas, U., Lemke, D., Mattila, K., Stickel, M., & Haas, M. 2004, A&A, 414, 69

Yi S., Demarque P., Kim Y. C., Lee Y. W., Ree C. H., et al. 2001, ApJS 136, 417

Zaritsky, D., Harris, J., Grebel, E. K., & Thompson, I. B. 2000, ApJ, 534, L53

Zaritsky, D., Harris, J., & Thompson, I. B. 1997, AJ, 114, 1002